American Journal of Applied and Industrial Chemistry
2019; 3(1): 9-14
http://www.sciencepublishinggroup.com/j/ajaic
doi: 10.11648/j.ajaic.20190301.12

Electrochemical Corrosion Study of Buried Pipeline Steel X20 Affected by Stray Current

Fangfang Xing[1], Chengtao Wang[2, *]

[1]School of Mechatronic Engineering, Xuzhou College of Industrial Technology, Xuzhou, China

[2]School of Mechatronic Engineering, Department of Mechanical Electronics, China University of Mining and Technology, Xuhou, China

Email address:
xzwangchengtao@163.com (Chengtao Wang)

[*]Corresponding author

To cite this article:
Fangfang Xing, Chengtao Wang. Electrochemical Corrosion Study of Buried Pipeline Steel X20 Affected by Stray Current. *American Journal of Applied and Industrial Chemistry.* Vol. 3, No. 1, 2019, pp. 9-14. doi: 10.11648/j.ajaic.20190301.12

Received: September 5, 2019; **Accepted**: September 27, 2019; **Published**: October 9, 2019

Abstract: With the continuous development of urban city, more and more subway lines are applied in the urban rail transit systems. During the daily operation of metro, the insulation performance between running rails and earth is gradually decreased. Thus, the stray current is generated at where the current flows out of the running rail. Stray current leakage and the corrosion caused by it are not negligible negative effects. Stray current corrosion will cause severe electrochemical corrosion to the metallic structures in and around the subway system, such as buried pipelines, running rails and concrete reinforcement etc. In view of the current situation of buried pipelines being affected by stray current corrosion, this paper starts with the stray current corrosion experiment of X20 pipeline steel. The experimental system was built up to simulate the stray current corrosion on the buried metallic pipeline. Electrochemical measurements including Tafel method and electrochemical impedance spectrum (EIS) were conducted in this study. Based on the measurement results and microscope morphology, the electrochemical corrosion process of X20 steel was discussed in detail Then the equivalent circuit model of the corrosion system was fitted and analyzed. It was found that the Nyquist plot of X20 corrosion system shows the characteristics of double capacitive reactance arc, and the corrosion system can be equivalent to a $R_s(CPE_{pore}R_{pore})(CPE_{dl}R_{ct})$ model. Finally, the stray current corrosion in the subway was introduced with engineering background, in which more influencing factors including microorganism, tube pressure, pH and water content value of soil, are pointed out for future research.

Keywords: Stray Current, Electrochemical Corrosion, X20 Steel, Pipeline Steel, Subway

1. Introduction

Stray current is regarded as a severe electrochemical phenomenon in the DC transit system, which was firstly studied from the perspective of its distribution model [1]. Stray current, however, is varied in the case of the subway locomotive constantly changing the operating position and traction current, which makes it difficult to accurately monitor [2, 3]. In the DC mass transit system, the running rails are employed as both the locomotive load bearing, guidance device and the traction return path. As shown in Figure 1, stray current generates from the traction current leakage from the running rails due to the deterioration of rail insulation performance, which will flow into the underground environment through the soil and flows out from the buried pipeline. The stray current corrosion is usually generated at where the current leave from the buried pipeline [4]. According to the basic principle of electrochemistry, the inflow region of stray current is usually called the cathode region, while the area where stray current outflows the pipeline is usually called the anode region. In the subway running rail and buried metallic pipeline, the spatial position of cathode area and anode area are relatively independent. Stray current corrosion is essentially due to the redox reaction of the metal medium in the anode region with the surrounding electrolyte, which will eventually lead to the conversion of the metal medium into metal ions [5].

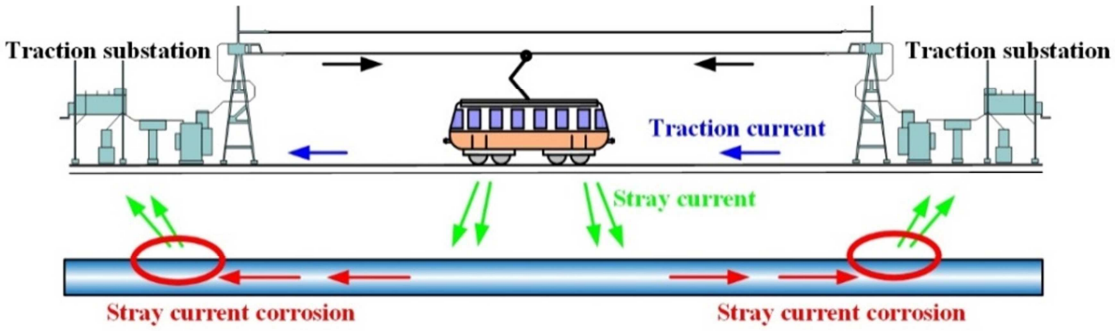

Figure 1. *Subway system and stray current corrosion.*

Stray current corrosion is a typical electrolytic corrosion that obeys Faraday's law. Stray current corrosion poses a serious safety threat to the media delivery in buried pipeline [6], especially for the flammable media such as oil, gas, aviation fuel, etc. There have been reports of related accidents of subway system due to stray current corrosion [7, 8]. In Hong Kong, corrosion perforation of gas pipes was caused due to stray current in the subway [9]. It has also been reported in the United States that stray current from cathodic protection systems have caused water pipe perforations in contact with the leakage point of the gasoline line, and the exposed water erodes the surface of the gasoline line to disable the cathodic protection [10]. Although the stray current leakage and its corrosion have been suppressed to a certain extent, in order to solve the stray current problem as much as possible, there is still much research value and space.

Many papers reported research results about stray current distribution modeling [11], stray current monitoring [12], stray current signal processing method [13, 14], electrochemical diagram of stray current corrosion [15], and protection and preventive measures for stray current corrosion [16] etc. Xu et al. built up the stray current distributing model considering the dynamic characteristics of locomotive and boundary conditions outside the traction interval [17]. Bertolini et al. analyzed the corrosion behavior of steel in concrete in the presence of stray current, and found that the stray current corrosion under DC excitation is far more dangerous than AC excitation [18]. Li et al. developed an integrated monitoring and prevention system for stray current in the subway, in which the distribution of stray current in metro and the corrosion of the metal structure in the whole line can be effectively monitored and preventive measures can be realized through drainage net system [19]. Cheng et al. studied CP potential under the DC interference, found that the CP potential was shifted to positive and negative directions in the anodic and cathodic zones [20].

X20 steel, as a typical kind of low-carbon steel, is widely applied in non-corrosive medium conveying pipeline. In this paper, the X20 pipeline steel was selected as the research object. The rest content of this paper is organized as follows. Firstly, the experimental process of this research was introduced. Then, the experimental results, including Tafel curve measurement, electrochemical impedance spectroscopy and surface morphology, was stated and discussed along with different affecting factors. In the next section, stray current in the subway system is introduced with engineering background. Finally, the conclusions were drawn and summarized.

2. Experimental

2.1. Material and Solution

The corrosion specimens utilized in this study were all cut from the X20 steel pipeline, the chemical composition of which is given in Table 1. The corrosion specimens are machined into the size of 20 mm×20 mm×7 mm through wire electrical discharge machining technology. The five faces of the corroded sample were sealed with silicone rubber, leaving a 400 mm^2 plane for stray current corrosion. Then the samples were grinded with sandpaper under different grades of 240, 400, 800, 1000, 1500, 2000, 2500, 3000, 5000 and 7000. All the specimens were washed with distill water and methanol, and drying in the air. The pretreated specimen is shown in Figure 2. The NaCl was employed as the corrosive medium in this study. All the test in this study was conducted in the inside environment of approximate 20°C.

Table 1. *Chemical composition of X20 steel corrosion specimen.*

C	Si	Mn	P	S	Ni	Cr	Cu	As
$\times10^{-2}$	$\times10^{-2}$	$\times10^{-2}$	$\times10^{-3}$	$\times10^{-3}$	$\times10^{-3}$	$\times10^{-3}$	$\times10^{-3}$	$\times10^{-3}$
19	20	36	19	8	60	90	30	7

2.2. DC Stray Current Corrosion and Tafel Polarization Curve Tests

The experimental system employed for this study is shown in Figure 2. The corrosion cell is powered by a controlled DC power source. The Tafel polarization curve measurements were conducted through CHI660E electrochemical workstation. The whole corrosion time for each specimen is 1h. The Tafel curve is measured every 10min. Three electrode system is utilized in this experiment, including a working electrode - X20 specimen, a counter electrode–Ti electrode, and a reference electrode–saturated calomel electrode (SCE), as shown in Figure 3. Apart from this, a same cathode electrode is placed opposite the working electrode to ensure the DC corrosion circuit. During the electrochemical testing, the test loop is completely independent of the applied DC corrosion loop, and the polarization curves of the corrosion

system are tested at different chloride ion concentrations. The potential range of each scan during Tafel curve test is 0.3 V above and below the open circuit potential, which is measured before the Tafel curve test. The scanning rate was set to 2 mV/s.

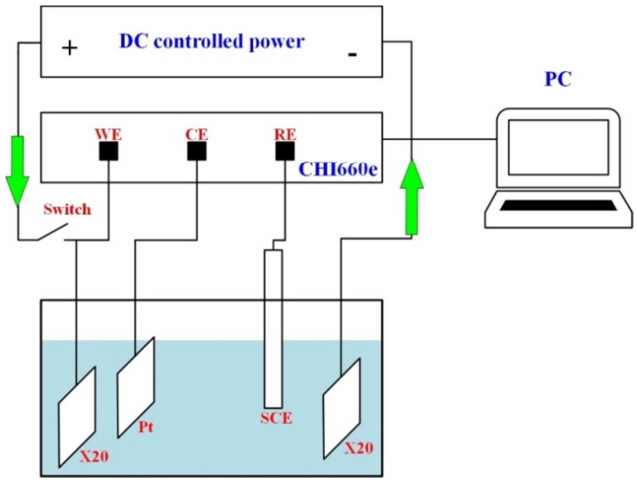

Figure 2. *Experimental system for the stray current corrosion of X20 pipeline steel.*

2.3. EIS Measurements

The EIS measurements were conducted by CHI660E electrochemical workstation. The total corrosion time and test interval of the EIS test were the same as the polarization curves. The EIS measurement was started after each specimen reaches a steady-state condition. A 5 mV testing potential is applied in the test. The high and low frequency is 0.01 and 100000 Hz respectively.

2.4. SEM Tests

Before the SEM scanning, the specimens are washed through the ultrasonic cleaner, and dried in the air after scrubbing with acetone. The SEM scanning was carried out by the FEI Quanta TM 250 scanning electron microscope, using the high vacuum mode.

3. Experimental Results and Discussion

3.1. Tafel Polarization Curve at Various Chloride Ion Concentrations

In the NaCl solution of 0.2 mol/L, the Tafel curve under different corrosion time is given in Figure 3. It can be seen from Figure 4 that the cathodic and anodic curve varies due to different ion concentrations. There is an exponential increase of current density in the polarization curve because the oxidation of steel electrode is generated in the anodic polarization zone, which correspond to the Bulter – Volmer equation. The polarization curves are different with various corrosion time due to the changing surface of the working electrode during the uniform corrosion process. The self-potential in Figure varies from -0.608 V to -0.575 V. Furtherly, the corrosion current density and linear polarization resistance can be obtained by a slope of polarization curve in the linear range near the self–corrosion potential.

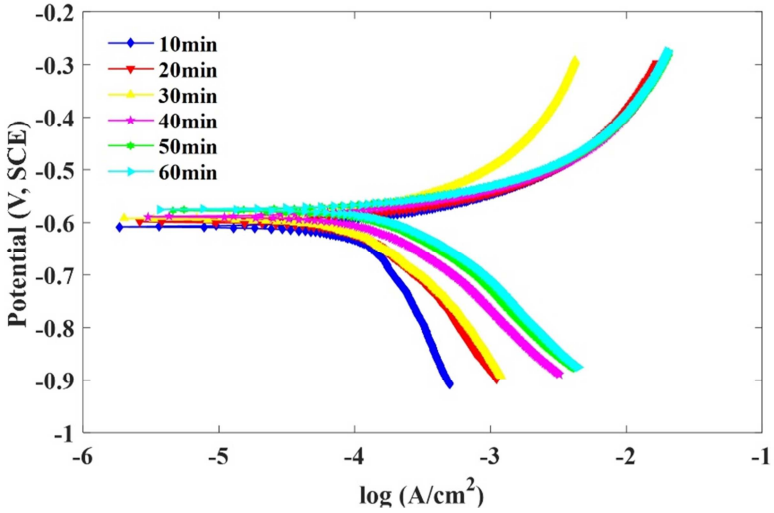

Figure 3. *Polarization curves of corroded samples under different chloride ion concentration.*

3.2. EIS Measurement Results and Analysis

When the X20 sample was corroded for 30 min, the EIS testing results under the ion concentration of 0.1 mol/L and the stray current density of 0.025 A/cm^2 is illustrated in Figure 4. According to the Nyquist plot, the EIS signal shows typical characteristics of dual capacity reactance. There regions can be observed in the Bode plot, which is low-frequency region, middle-frequency region and high frequency region. There is a small arc in the high-frequency area and a bigger arc in the low-frequency area. When the frequency is higher than 10^2 Hz, the resistance in the Bode plot stays at a lower level and doesn't change much with the increasing frequency. When the frequency drops from 10^2 Hz, the resistance of the whole corrosion system increases. The two crests in the phase diagram indicate two capacitive responces.

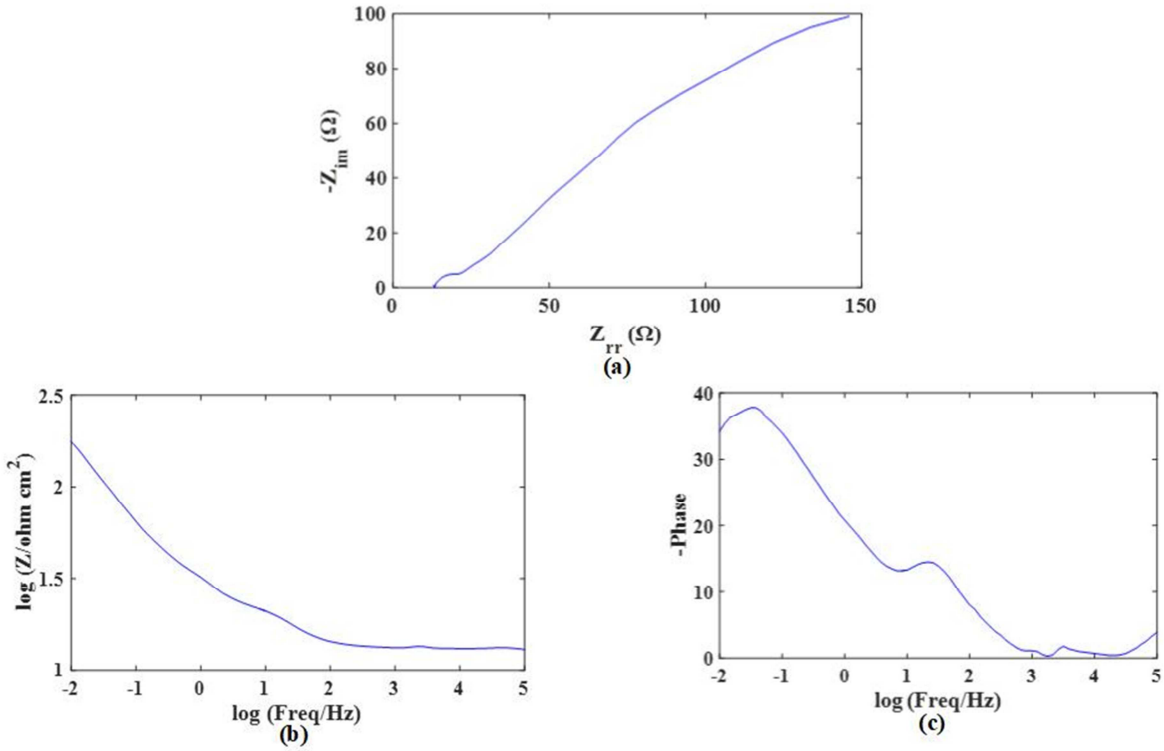

Figure 4. *Nyquist plot and Bode plot of X20 steel corroded by stray current.*

Equivalent electric circuit $R_s(CPE_{pore}R_{pore})(CPE_{dl}R_{ct})$ is employed to fit the EIS data, where R_t, R_{ct}, R_{pore}, CPE_{dl} and CPR_{pore} are the solution resistance, charge transfer resistance, porous corrosion product layer resistance, constant phase element of corrosion product X20 interface and porous corrosion product layer, respectively. The fitting results of the Nyquist plot and the equivalent electrical circuit in shown in Figure 5. The fitting results show good agreement with the tested Nyquist, which is believed to represent the corrosion system.

Table 2. *Electrical parameters of the equivalent circuit.*

R_{sol} ($\Omega\cdot cm^2$)	R_{pore} ($\Omega\cdot cm^2$)	CPE1-T ($\mu\Omega^{-1}\cdot cm^2\cdot s^P$)	CPE1-P	R_{ct} ($\Omega\cdot cm^2$)	CPE2-T ($\mu\Omega^{-1}\cdot cm^2\cdot s^P$)	CPE2-P
13.103	5.843	0.0016995	0.94684	723.9	0.024162	0.55001

3.3. Corrosion Morphology

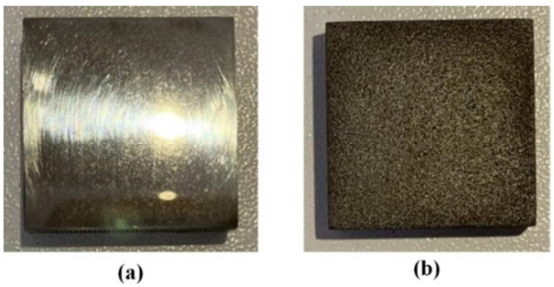

Figure 5. *Macroscopical morphology of X20 sample: (a) un-corroded; (b) 0.0250 A/cm^2-4 mol/L Nacl-1 h.*

Figure 5 shows the macroscopical morphology of un-corroded and corroded X20 steel specimens in the sodium chloride solution. Compared to the un-corroded specimen, it can be clearly seen from Figure 5 that the surface of corrosion sample becomes rougher and dimmer. Due to the loss of metal caused by stray current corrosion, a lot of pit-like peeling occurs on the metal surface.

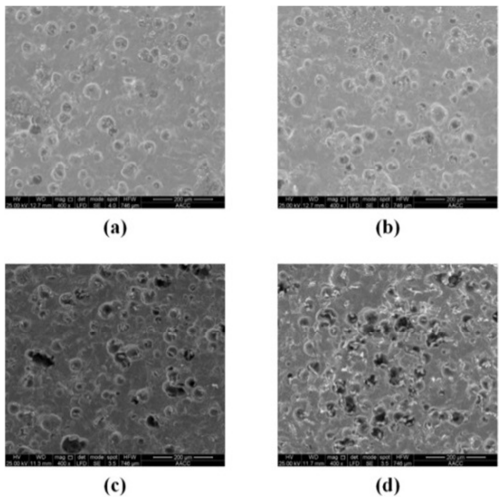

Figure 6. *Optical view of the morphology of corroded X20 specimens under different chloride ion concentrations: (a) 0.1 mol/L; (b) 0.2 mol/L; (c) 0.3 mol/L; (d) 0.4 mol/L.*

Figure 6 shows the microscopic morphology of X20 pipeline steel for 2h stray current corrosion in the sodium chloride solution. Due to the peeling of the metal caused by the electrochemical corrosion, a various of pit-like and pore-like structures appear on the metal surface. As can be seen from Figure 6, with the increase of chloride ion concentrations, the pit-like and pore-like structures increases. According to the scanning results of SEM, it can be concluded that the chloride ion is the main factor pit and pore flaking on metal surface.

4. Stray Current Corrosion in the Subway

The essence of stray current in the subway is the same as the experiment conducted above. However, the stray current corrosion in the DC mass transit system is affect by other more factors, which is not completely considered in the electrochemical experiment. According to the existing research results, the stray current corrosion often interacts with microorganisms in buried metals in the underground environment, which often exacerbates corrosion of buried metals. Besides, the tube pressure in the buried pipeline also has an effect on stray current corrosion, which has been proved in the related literature [21]. Besides, the corrosion degree of buried pipeline increases with the increase of soil water content, but when the soil water content reaches saturation, the corrosion will be difficult to occur. When the buried pipelines are in the highly acidic soil with pH value below 4, it will be strongly corroded. If it acts with stray current, electrochemical corrosion will be further intensified. It should also be pointed out that the stray current has dynamic characteristics due to the influence of the traction current, which needs to be realized in future electrochemical corrosion experiments.

5. Conclusion

In this paper, the electrochemical characteristics of X20 steel under the excitation of stray current is studied from the perspective of Tafel curve and EIS measurement. With the corrosion time of 1 h, the corrosion current density increases with the corrosion time. Correspondingly, the linear polarization resistance decreases. Based on the scanning results of SEM, the chloride ion is the main factor pit and pore flaking on metal surface. With the increase of chloride ion concentration, the number of pit-like and pore-like structures on the specimen surface increases.

The equivalent circuit X20 corrosion system under the effect of stray current is fitted to be a $R_s(CPE_{pore}R_{pore})(CPE_{dl}R_{ct})$ model. The corrosion system is composed of electrolyte environment, corrosion product layer and the interface.

Based on the further understanding of corrosive effect of stray current on X20 steel,

more factors need to be considered in the future electrochemical experiment. In this way, it is possible to simulate stray current corrosion that is closer to the operating conditions.

References

[1] Sim, W. M., & Chan, C. F. (2004). Stray current monitoring and control on Singapore MRT system. International Conference on Power System Technology. IEEE.

[2] Memon, S. A., & Fromme, P. (2014). Stray current corrosion and mitigation: a synopsis of the technical methods used in dc transit systems. IEEE Electrification Magazine, 2 (3), 22-31.

[3] Mo, S., Yang, S., Lu, X., Zhang, J., Liu, Y., & Liu, X., et al. (2013). Investigation of Dynamic Stray Current Interference from Direct Current System with City Pipelines. International Conference on Pipelines & Trenchless Technology.

[4] Alamuti, M. M., Nouri, H., & Jamali, S. (2011). Effects of earthing systems on stray current for corrosion and safety behaviour in practical metro systems. IET Electrical Systems in Transportation, 1 (2), 69-0.

[5] Wang, J., Li, Z., Cui, G., Liu, J. G., Kong, C., & Wang, L., et al. (2019). Corrosion behaviors of X70 steel under direct current interference. Anti-Corrosion Methods and Materials.

[6] Chen, Z. G., Qin, C. K., Tang, J. X., & Zhou, Y. (2013). Experiment research of dynamic stray current interference on buried gas pipeline from urban rail transit. Journal of Natural Gas Science and Engineering, 15 (Complete), 76-81.

[7] Law, D. W., Cairns, J., Millard, S. G., & Bungey, J. H. (2004). Measurement of loss of steel from reinforcing bars in concrete using linear polarisation resistance measurements. NDT and E International, 37 (5), 381-388.

[8] Ibrahim, & Emad, S. (1999). Corrosion control in electric power systems. Electric Machines & Power Systems, 27 (8), 795-811.

[9] Brichau, F., Deconinck, J., Driesens, T. (1996) Modeling of underground cathodic protection stray currents. Corrosion, 52: 480-487.

[10] Uhlig, H. H., & King, C. V. (1972). Corrosion and corrosion control. Journal of The Electrochemical Society, 119 (12), 327C.

[11] Yu, J. G., & Goodman, C. J. (1990). Modelling of rail potential rise and leakage current in DC rail transit systems. IEEE Colloquium on Stray Current Effects of Dc Railways & Tramways. IET.

[12] Chen, Z., Qin, C., Zhang, Y., & Guo, C. (2010). Design and application of a stray current monitoring system. International Conference on Computer. IEEE.

[13] K. Żakowski, & W. Sokólski. (1999). 24-hour characteristic of interaction on pipelines of stray currents leaking from tram tractions. Corrosion Science, 41 (11), 2099-2111.

[14] Darowicki, K., & Zakowski, K. (2004). A new time–frequency detection method of stray current field interference on metal structures. Corrosion Science, 46 (5), 0-1070.

[15] Liwei, Z., Bingkun, Y., Min, L., Jiaxiu, H. U., & Zhouhai, Q. (2016). Stray current corrosion behavior of q235 carbon steel grounding material. Journal of Hebei University (Natural Science Edition).

[16] Jiang, L., Hua, T., & Xue, Y. H. (2002). Protection of stray current corrosion in metro. Journal of Building Materials.

[17] Xu, S. Y., Li, W., & Wang, Y. Q. (2013). Effects of vehicle running mode on rail potential and stray current in dc mass transit systems. IEEE Transactions on Vehicular Technology, 62 (8), 3569-3580.

[18] Bertolini, L., Carsana, M., & Pedeferri, P. (2007). Corrosion behaviour of steel in concrete in the presence of stray current. Corrosion Science, 49 (3), 0-1068.

[19] Li, W., & Yan, X. (2001). Research on integrated monitoring and prevention system for stray current in metro. Journal of China University of Mining & Technology, 11 (2), 221-228.

[20] S. Qian, Y. F. Cheng, (2017). Accelerated corrosion of pipeline steel and reduced cathodic protection effectiveness under direct current interference, Constr. Build. Mater. 148 675-685.

[21] Evans, C., Leiva-Garcia, R., & Akid, R. (2018). Strain evolution around corrosion pits under fatigue loading. Theoretical and Applied Fracture Mechanics, 95, 253-260.